RESIDUAL STRESS MEASUREMENT ON WELDED Q345GJ STEEL H-SECTIONS BY SECTIONING METHOD AND METHOD IMPROVEMENT

Bo Yang[1, 2], Shidong Nie[1, 2], Shao-Bo Kang[1, 2], Gang Xiong[1, 2, *], Ying Hu[1, 2], Jubo Bai[1, 2], Weifu Zhang[1, 2] and Guoxin Dai[1, 2]

[1] *Key Laboratory of New Technology for Construction of Cities in Mountain Area (Chongqing University), Ministry of Education, Chongqing 400045, China*
[2] *School of Civil Engineering, Chongqing University, Chongqing 400045, China*
**(Corresponding author: E-mail:* 195704148@qq.com*)*

Received: 7 December2015; Revised: 13 April 2016; Accepted: 1 May 2016

ABSTRACT: High-performance structural steel has attracted a lot of attention in the past decade and been widely used in many landmark building structures, such as the National Olympic Stadium, the new CCTV Headquarters, and the Canton Tower in China. However, their structural performance has not been fully studied yet. Among all parameters, residual stress is one of the most important mechanical imperfections, which can reduce the stability resistance of steel structures. This paper presents an experimental investigation on the residual stress in welded H-sections made of high-performance steel Q345GJ by using sectioning method. Besides, a simple yet accurate method was proposed for determining the residual stress of curved strips. Comparisons between residual stress profiles obtained by different methods suggested that the proposed method was in good agreement with other ones. Test results showed that the magnitudes of residual stress in welded Q345GJ H-sections was significantly different from that predicted by existing models. Finally, suggestions were made for welded Q345GJ steel H-sections in accordance with experimental results.

Keywords: Q345GJ steel, Welded H-sections, Residual stress, Sectioning method, Curve correction, Straightening method

DOI: 10.18057/IJASC.2017.13.1.5

1. INTRODUCTION

Since this century, the number of large-span and high-rise buildings is increasing rapidly worldwide. In these types of structures, high performance structural steel has been extensively used due to high levels of vertical and horizontal loads. As a typical high-performance steel, high-strength steel with tensile strength of 460 MPa to 1000 MPa has been employed in construction practices in Japan [1], Europe [2], the USA [3] and Australia [4]. However, with increasing steel strength, material properties such as the reduction of plastic deformation capacity, poor weldability and low impact toughness become more critical which may lead to brittle failure [5]. Therefore, merely increasing tensile strength of steel may not meet the requirements for the design of steel structures, in particular for large-span or super high-rise buildings.

To overcome the main weaknesses of high-strength steel, high-performance SN structural steel has been developed and incorporated in Japanese standard since 1994 [6]. More stringent requirements are specified for SN steel than normal one to ensure full plastic deformation of steel structures under strong earthquakes. In addition, lower carbon equivalent ($\leq$0.46) in SN steel enables it to achieve better weldability. In the USA, American structural steel A992 [7] shows similar performance to SN steel and it has been widely used in building structures, especially in the areas with high seismic intensity [8, 9]. In China, another type of high-performance structural steel, designated as GJ, has been included in the national standard of "Steel plates for building structure"

(GB/T19879-2005) [10]. Compared with conventional steel in the standards of "Carbon structural steels" [11] and "High-strength low-alloy structural steels" [12], this type of structural steel is more appropriate for use in large-span or high-rise structures due to its lower content of harmful non-metallic elements like sulphur and phosphorus, smaller yield-to-tensile strength ratio, less scatter of yield strength, lower thickness effect on yield strength and better weldability [13]. High-performance GJ steel, mainly Q345GJ, has been utilised in many landmark projects, such as the National Olympic Stadium (the Bird Nest Stadium) [14], the CCTV Headquarters in Beijing [15], and the Canton Tower [16]. However, the same design methods and design values as that for conventional steel are recommended for GJ steel [17]. Indeed, there can be significant differences between GJ and conventional steels in terms of the stability resistance, and thus, the advantages of GJ steel over conventional steel have not been fully taken in current design due to the lack of test data.

Among all parameters, residual stress is one of the most important mechanical imperfections, which can reduce the stability resistance of steel structures. Besides, it can also affect the machining accuracy of weldment and result in stress corrosion cracking [18]. In order to provide fundamental experimental data for further study on the stability resistance of welded GJ steel H-beams under vertical load, it is necessary to quantify the residual stress distribution in the sections through experimental tests.

This paper presents an experimental study on the residual stress in welded Q345GJ steel H-sections. In the experimental programme, sectioning method was used to quantify the residual stress distribution in four welded Q345GJ H-sections. Comparisons were made among different methods for curve corrections. Besides, a new method was proposed for curved strips whereby correction process can be greatly simplified. Experimental results suggested that the residual stress distribution model in welded Q345GJ H-sections was different from that in conventional steel sections. This study serves as the basis of further experimental and numerical investigations on the stability resistance of Q345GJ steel beams subject to vertical loads.

2. SECTIONING METHOD FOR RESIDUAL STRESS MEASUREMENT

Several methods can be used to determine the residual stress in steel sections, namely, sectioning method, hole-drilling method, X-ray method and ultrasonic method [19].Among all the methods, the sectioning method is easy and simple for use due to its good operability and high accuracy. It can also be used to verify the accuracy of other measuring methods [20, 21].

In the sectioning method, internal residual stresses on a section are released by cutting the section into a number of small strips. By measuring the change in the strip length before and after cutting, the average residual stress along a specific length of the section can be quantified in accordance with Hook's Law. Accordingly, the residual strain can be calculated from the following equation.

$$\varepsilon_r = \varepsilon_1 - \varepsilon_{T1} = \frac{L_f - L_i}{L_i} - \frac{L_{Tf} - L_{Ti}}{L_{Ti}} \quad (1)$$

where ε_r is the average residual strain over a specific length; ε_1 is the total strain due to relaxation and temperature change; ε_{T1} is the strain induced by temperature change; L_i is the initial gauge length before cutting; L_f is the final gauge length after cutting; L_{Ti} is the initial gauge length of reference strip; and L_{Tf} is the final gauge length of reference strip.

Thus, the residual stress can be quantified from Eq. 2.

$$\sigma_r = -E\varepsilon_r \quad (2)$$

where σ_r is the average residual stress and E is the elastic modulus.

By means of the sectioning method, a large number of experimental studies have been conducted on the residual stresses in different types of steel. As for conventional steel, Alpsten and Tall [22] experimentally investigated the residual stress in welded sections of different dimensions and welding processes and analysed the effects of various parameters on the residual stress. Similar tests were also conducted by Tebedge et al. [20]. Besides, Wang et al. [21] proposed a simplified residual stress distribution model based on test results For high-strength steel, Rasmussen and Hancock [23, 24] quantified the residual stress of welded H and cruciform sections of 690 MPa steel by using the sectioning method. Wang et al. [25, 26] and Ban et al. [27-29] determined the residual stress distributions in various type of welded sections made of high-strength steel, such as H and box sections. In accordance with the experimental results, a new set of residual stress distribution models was proposed for steel sections with different dimensions. For high-performance structural steel, experimental investigations were conducted by Spoorenberg et al. [30] on the residual stress in wide flange quenching and self-tempering 460 MPa steel sections. However, limited test data are available for welded GJ steel sections to date. Therefore, experimental tests are needed to determine the residual stress distribution model in welded GJ steel sections.

3. EXPERIMENTAL PROGRAMME

3.1 Specimen Design and Manufacture

In the experimental programme, four welded Q345GJ steel H-sections with different dimensions were tested by using the sectioning method, as shown in Figure 1. Table 1 summarises the details of specimens. Specimens with fillet welds between steel plates were fabricated by flame-cut plates and submerged arc welding. The four specimens were classified into two categories. One category contained two doubly-symmetric sections with blind holes drilled on the outer surface only, whereas the other included one doubly-symmetric section and one singly-symmetric section with through holes on both outer and inner surfaces.

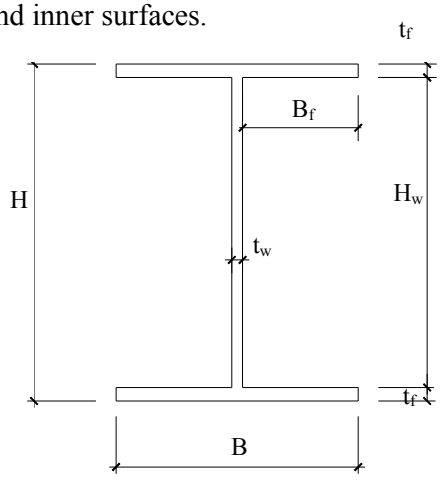

Figure 1. Schematic of sectional dimensions

Table 1. Welded H-sections of Q345GJ steel

Hole type	Specimen	Sectional dimension	H (mm)	B (mm)	t_w (mm)	t_f (mm)	H/B	B_f/t_f	H_w/t_w
Blind hole	H1	300*200*8*10	300	200	8	10	1.5	9.6	35
	H2	400*200*8*10	400	200	8	10	2.0	9.6	47.5
Through hole	H3	400*200*8*10	400	200	8	10	2.0	9.6	47.5
	H4	350*220(180)*8*10(8)	350	220/180	8	10/8	1.59/1.94	13.25/10.75	41.5

3.2 Material Properties

Prior to testing, tensile coupons were cut per Chinese standard GB/T GB2975-1998 [31] and tested in accordance with GB/T 228.1-2010 [32]. Figure 2 shows the dimensions of the coupons. Table 2 includes the material properties of steel, including Young's modulus E, yield strength R_{eH} and ultimate tensile strength R_m.

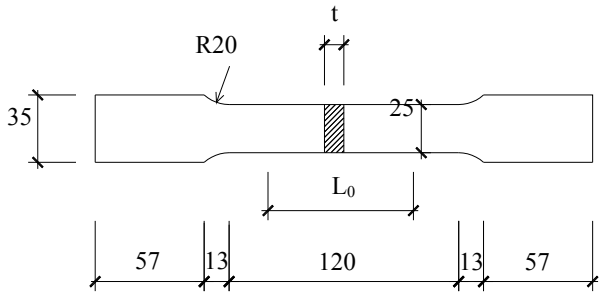

Figure 2. Geometry of tensile coupons

Table 2. Material properties of Q345GJ

Thickness of plates t (mm)	R_{eH} (MPa)	R_m (MPa)	E (GPa)
10	397.6	539.9	209.2
8	457.8	600.8	204.8

3.3 Sectioning Process

Sectioning of welded Q345GJ H-sections was conducted following the procedure recommended by Ziemian [19] and Alpsten and Tall [22]. The selected section for residual stress measurement was at least 1.5 times the section depth away from both ends in order to eliminate the end effect. Considering both accuracy and efficiency, the width of strips in the flanges and at the edges of the web was about 10 mm, while the width was adjusted to 15 mm in the middle of the web. Two gauge holes with a distance of 250 mm (Whitttemore strain gauge length) were drilled along the centre line of each strip. Figure 3 shows the details of blind and through holes. The specimens were

sectioned into small strips with specific length and widths by using wire electrical discharge machining, as shown in Figure 4, which released little heat during sectioning. The distance between the two holes on each strip was measured by using Whitttemore strain gauge with an accuracy of 0.001 mm before and after sectioning. Meanwhile, a reference strip with the same material and dimensions was measured to eliminate the temperature effect. To minimise the errors, each strip was measured for three times. For curved strips, the offset of steel strips from the original axis was measured for curve corrections on a high-precision measuring table.

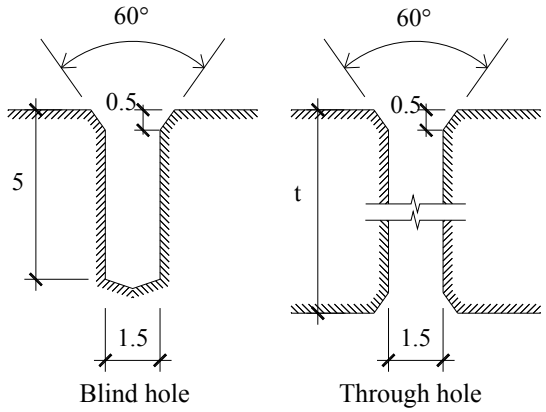

Figure 3. Dimension of gauge holes

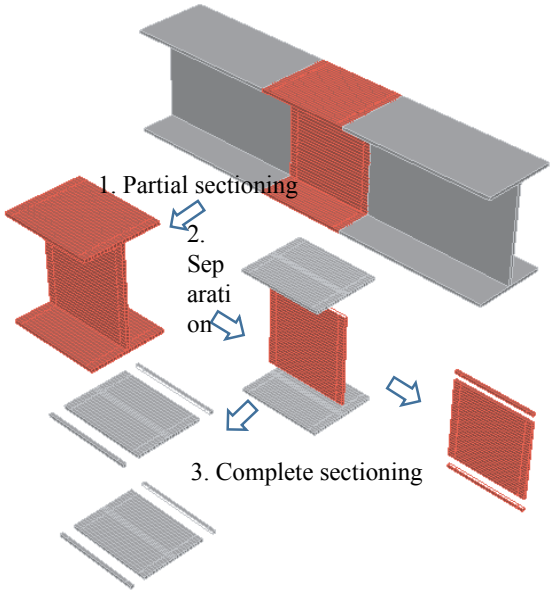

Figure 4. Procedure for sectioning

4. CORRECTION OF RESIDUAL STRESS

After sectioning, steel strips near the flame-cut edges and welds showed significant out-of-plane curvature. On this condition, the measured strip length was only the chord length rather than arc length, as shown in Figure 5. Thus, corrections had to be made in calculating the strain. Several correction methods have been proposed to take account of the curvature.

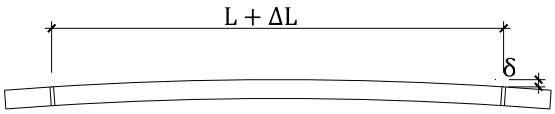

Figure 5. Geometry of curved strips

4.1 Curve correction Method

In accordance with test results, Tebedge and Tall [22] suggested a correction equation, as expressed in Eq. 3, and pointed out that the axial stress was the average value of top and bottom stresses.

$$\Delta\varepsilon = \frac{(\delta/L)^2}{6(\delta/L)^4 + 1} \tag{3}$$

where L is the gauge length of steel strips and δ is the offset to gauge length (see Figure 5). The equation has been widely used for calculating residual stresses in steel sections [33, 34].

Besides, Cui [35] assumed a parabolic curve and derived a correction equation, as expressed in Eq. 4.

$$\Delta\varepsilon = \left[40\left(\frac{\delta}{L}\right)^2 - 96\left(\frac{\delta}{L}\right)^4\right]/15 \tag{4}$$

However, Sherman [36] suggested that, for a long prismatic member, the residual stress did not vary along its length and the curve was a portion of a circular curve in the residual stress measurement in tubular members. In order to obtain the strain relaxation at the middle-thickness layer of a strip, three corrections were required, including the final measurement along the chord instead of the arc ε_s, the misalignment of the conical extensometer point and gauge hole axis ε_h, and the difference between the outer surface and middle-thickness layer ε_t. Moreover, another correction ε_n due to lateral bending was introduced by the Structure Stability Research Council [37]. Therefore, four corrections had to be considered in residual stress calculations as follows.

$$\varepsilon_s = \frac{8}{3}\left(\frac{\delta}{L}\right)^2 \tag{5}$$

$$\varepsilon_h = \frac{4d\delta}{L^2}\tan\frac{\alpha}{2} \tag{6}$$

$$\varepsilon_t = \frac{4t\delta}{L^2} \tag{7}$$

$$\varepsilon_n = \frac{8}{3}\left(\frac{\delta_1}{L}\right)^2 \tag{8}$$

where δ_1 is the tortuosity sagittal height of lateral bending, d is the diameter of the contact edge hole, α is the internal angle of the extensometer gauge point, and t is the strip thickness.

The first two correction methods only consider the difference between chord and arc. Comparatively, more influential parameters are taken into account in the circular correction method proposed by Sherman [36]. If only the difference between chord and arc is taken into account, Eqs. 3, 4 and 5 provide substantially different results. Figure 6 shows the comparison of calculated

values from the equations. Among the three equations, Eq. 3 gives the smallest values, as shown in Figure 6, whereas the values obtained from Eqs. 4 and 5 are nearly identical. Furthermore, the discrepancy between Eqs. 3 and 4 or 5 increases with increasing δ/L. For instance, the difference is less than 5 MPa when δ/L is 1/250. However, the value reaches up to 90 MPa, if δ/L is equal to 4/250.

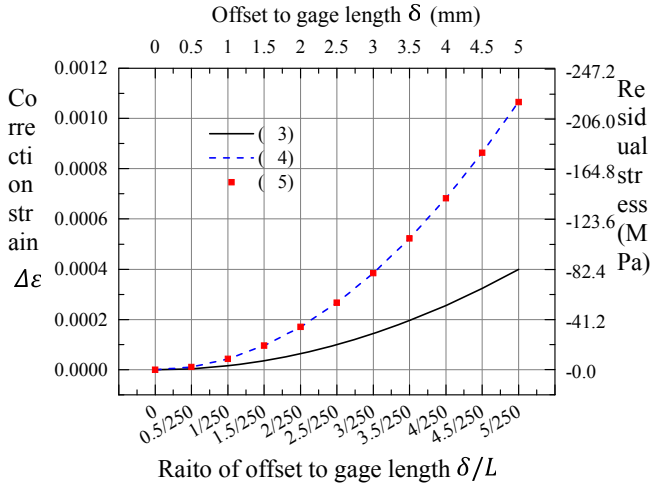

Figure 6. Comparison between different correction methods

Besides, in Sherman's circular curve correction method, the residual stress at the middle-thickness layer can be calculated from the measurement on one surface. Thus, this correction method is particular useful for closed sections like box and circular sections, as measurements on the inner surface cannot be easily made. Total circular curve correction is the combination of Eqs. 5, 6, 7 and 8. When a convex surface is measured, the total correction can be determined from Eq. 9.

$$\Delta\varepsilon = \varepsilon_s + \varepsilon_n - \varepsilon_h - \varepsilon_t \quad (6)$$

However, for a concave surface, the total circular curve correction becomes

$$\Delta\varepsilon = \varepsilon_s + \varepsilon_n + \varepsilon_h + \varepsilon_t \quad (7)$$

Calculations suggest that ε_t is the most critical parameter in determining $\Delta\varepsilon$. Besides, the calculated ε_t from Eq. 6 is largely dependent on the measurements of strip thickness t and arc offset δ. However, the offset cannot be easily measured in experimental tests. Therefore, it is preferred to measure on both surfaces of strips and calculate the average stress if possible.

4.2 Residual Stress Results

Figure 7 shows the calculated residual stressed. For specimens H1 and H2, measurements were only made on the out surface through blind holes and corresponding residual stress at the middle-thickness layer was calculated by using the circular curve correction method, as shown in Figures 7(a) and (b). However, through holes were prepared for specimens H3 and H4 and the circular curve correction method was used for both surfaces. The residual stress at the middle-thickness layer could be approximated by the average value of stresses on the outer and inner surfaces, as shown in Figures 7(c) and (d). It is noteworthy that the residual stresses on the outer and inner surfaces of flanges were quite different from each other. High compressive stresses

were obtained on the outer surface near the flange tip, whereas tensile stresses were on the inner surface. This was mainly attributed to the bending of these strips after sectioning. However, the residual stresses at the middle-thickness layer, obtained from the outer surface, inner surface and their average values, were close to one another. It indicates that results of specimens H1 and H2 could still be reliable, even though they were only calculated from the measurements on the outer surface.

5. STRAIGHTENING METHOD

When subject to pure bending, fibres of a slender beam are shortened on one surface and elongated on the other. At the neutral layer, the fibre length remains unchanged. As a result, the final length of a curved strip can be determined by straightening and the residual stress at the middle-thickness layer can be directly measured without any curve corrections.

Figure 8 shows the apparatus for straightening curved strips. By using a customised L-shaped marble table board with a flatness of 0.01 mm, the curve strip was placed at the re-entrant corner of the board, and then was straightened when two orthogonal surfaces of the strip clung tightly to the standard planes by using several G-clamps. Finally, the total length of the middle-thickness layer could be measured. Figure 9 shows the comparisons between residual stresses by straightening and the circular curve correction. Reasonably good agreement is obtained in terms of the residual stress distribution and magnitudes.

Residual stresses on each section should be self-equilibrated and the closing error of the stresses should be zero. Therefore, to evaluate the accuracy of the measured residual stresses, a closing error index σ_{err} is defined as follows.

$$\sigma_{err} = \left[\sum_{i=1}^{n} A_i \cdot \sigma_{ri}\right] / \sum_{i=1}^{n} A_i \tag{8}$$

where A_i is the cross-sectional area of a strip, σ_{ri} is the value of residual stress along the strip, and n reprents the number of strips.

Figure 10 shows the closing error indexes of residual stresses obtained from the two methods including the circular curve correction and straightening methods. The stress error indexes of the four sections were around zero and the maximum value was only 12.5 MPa, about 3.6% of the nominal yield strength. It indicates that both the circular curve correction and straightening methods yield good accuracy on residual stresses. Hence, in the following section, the mean value of residual stresses obtained from these two methods are used for determining the residual stress profile.

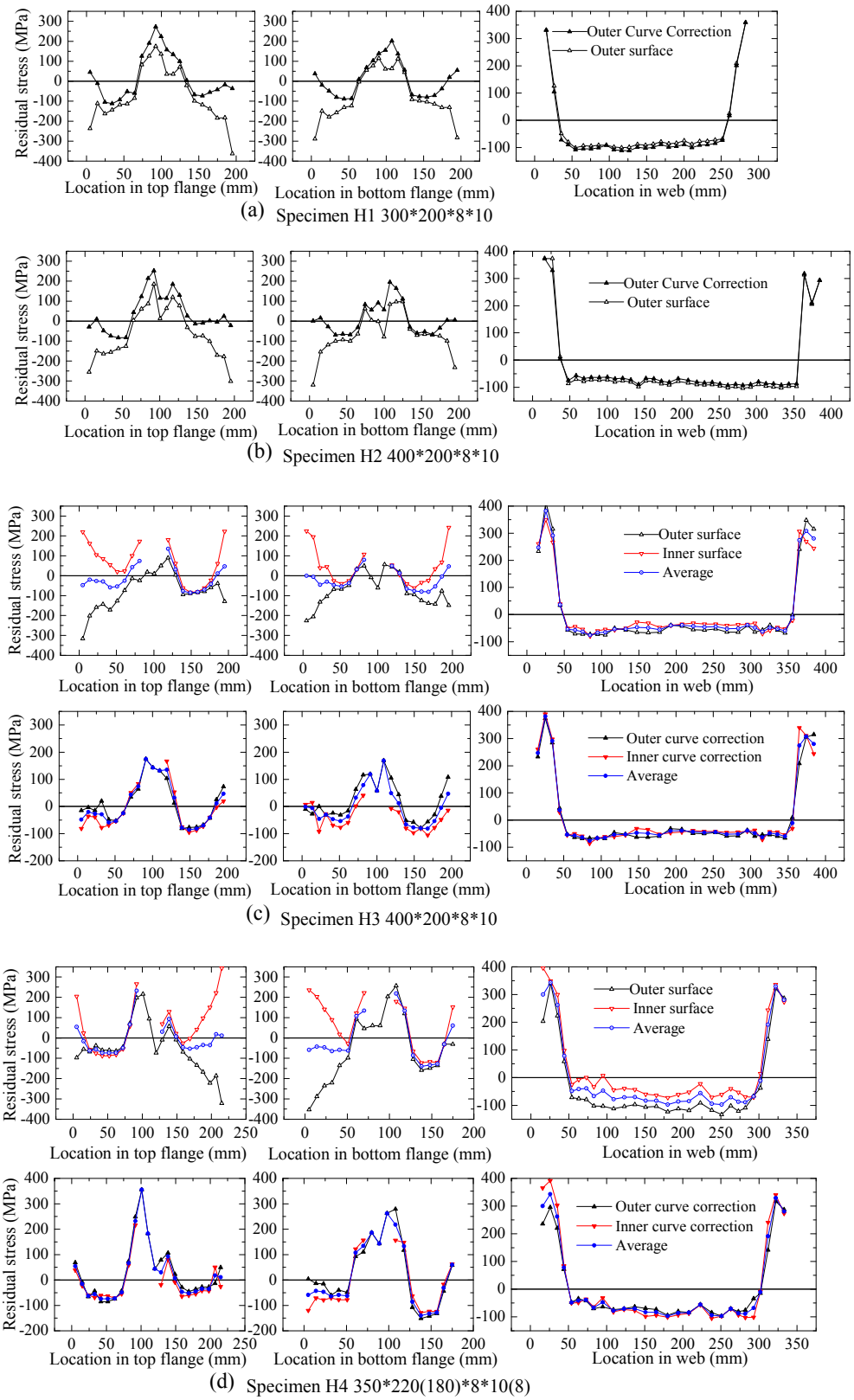

Figure 7. Residual stress distributions

Figure 8. Setup for straightening curved strips

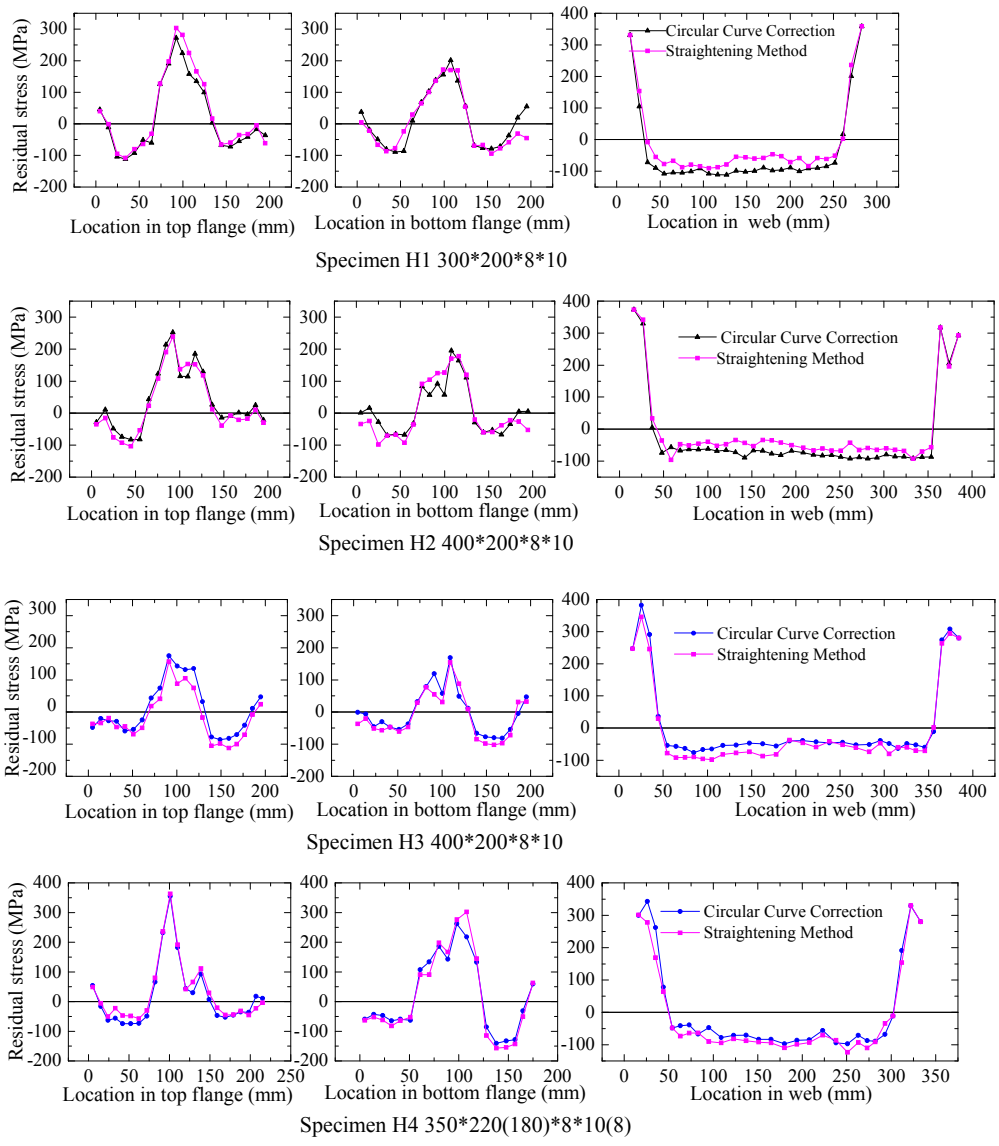

Figure 9. Comparison between residual stresses by correction

6. RESIDUAL STRESS PROFILE

The residual stress profile of welded Q345GJ steel sections is similar to that of conventional steel sections, as shown in Figure 9. The main characteristics of residual stresses are discussed as follows.

(1) A W-shaped bond stress profile was observed in the flange. In most cases, the flange tip was under tension with limited tensile stresses. In the middle of the flange were high tensile residual stresses, with the maximum value less than the nominal yield strength, except for the top flange of specimen H4. Compressive residual stresses were distributed at other regions of the flange, with the maximum value of about 100 MPa. Due to considerable bending of strips near the flange tip, residual stresses on the outer and inner surfaces were significantly different from each other.

(2) Tensile residual stresses with large gradient were measured near both ends of the web, but the maximum value was still less than the nominal yield strength. Compressive residual stresses with a peak value of 80 MPa were stable in the middle portion of the web.

Table 3 summarises the residual stresses at specific locations of welded H-sections. In the table, σ_{ft1}, σ_{ft2}, σ_{ft3} and σ_{ft4} denote the tensile residual stresses at the flange tips; σ_{fc1}, σ_{fc2}, σ_{fc3} and σ_{fc4} signify the maximum compressive values in the flanges; σ_{fwt1} and σ_{fwt2} represent the maximum tensile residual stresses in the flanges near the welds; σ_{wt1} and σ_{wt2} denote the maximum tensile stresses at the edges of the web; and σ_{wc} represents the average compressive stress in the middle of the web.

Table 4 lists the characteristic values of residual stresses in welded H-sections, which represent the average values of peak residual stresses. For example, σ_{ft} denotes the average value of four peak residual stresses at the four flange tips of H-sections. With these values, the effect of cross section on the residual stresses in the web and flanges can be studied. Specimens H1 and H2 had the same dimensions except for the web height, 280 mm and 380 mm, respectively. Almost the same characteristic tensile residual stresses were obtained in the web and flanges near the welds. However, the characteristic compressive stress (82.6 MPa) in the web of H1 was 23.5% greater than that (66.9 MPa) of H2. Besides, the characteristic compressive stress (86.7 MPa) at the flanges of H1 was 41.4% greater than that (61.3 MPa) of H2. The results indicate that during the cooling stage after welding, the section with higher web had a larger area to equilibrate shrinking stresses, which resulted in smaller compressive residual stresses. Therefore, the web and flanges were affected by each other, which is different from the assumption in many existing residual stress distribution models.

As a singly-symmetric section, H4 showed obvious asymmetry of residual stresses in the flanges, as included in Table 3. The maximum tensile residual stress in the top flange was 359.0 MPa, around 33.6% larger than that (268.8 MPa) in the bottom flange. Besides, the average peak compressive residual stress in the bottom flange was around 2 times the value in the top flange.

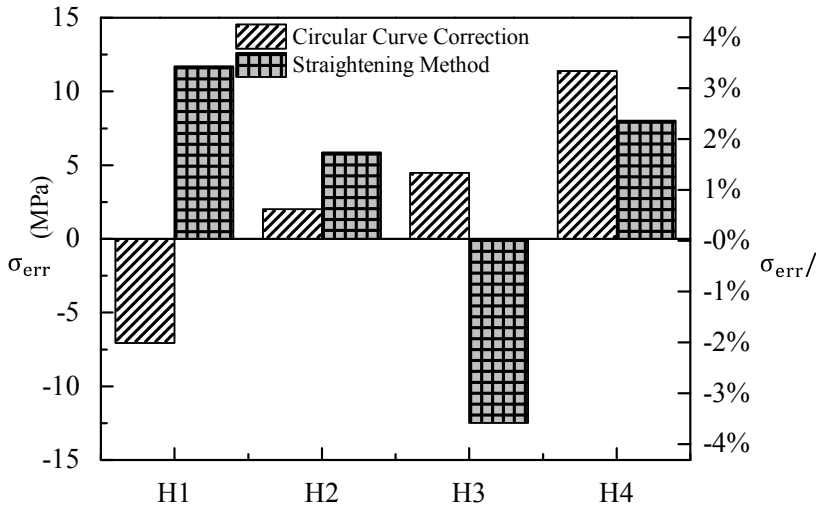

Figure 10. Residual stress closing error indexes of different methods

Table 3. Residual stresses at specific locations of welded H-sections

Specimen	In the flange (MPa)										In the web (MPa)		
	σ_{ft1}	σ_{ft2}	σ_{ft3}	σ_{ft4}	σ_{fwt1}	σ_{fwt2}	σ_{fc1}	σ_{fc2}	σ_{fc3}	σ_{fc4}	σ_{wt1}	σ_{wt2}	σ_{wc}
H1	42.3	-48.8	20.6	4.8	287.6	185.6	-109.9	-66.7	-83.5	-86.8	330.9	358.4	-82.6
H2	-32.0	-26.1	-16.7	-23.8	245.6	182.8	-93.5	-11.2	-80.3	-60.3	373.4	292.6	-66.9
H3	-42.3	35.4	-18.8	39.4	166.3	161.3	-61.1	-97.0	-57.4	-90.9	364.0	301.3	-61.8
H4	51.5	3.7	-60.8	61.7	359.0	268.8	-65.0	-48.9	-73.7	-148.8	310.5	329.5	-85.7

Table 4. Characteristic residual stresses at specific locations of welded H-sections

Specimen	In the flange (MPa)			In the web (MPa)	
	σ_{ft}	σ_{fwt}	σ_{fc}	σ_{wt}	σ_{wc}
H1	4.7	236.6	-86.7	344.6	-82.6
H2	-24.6	214.2	-61.3	333.0	-66.9
H3	3.4	163.8	-76.6	332.6	-61.8
H4	14.0	313.9	-84.1	320.0	-85.7

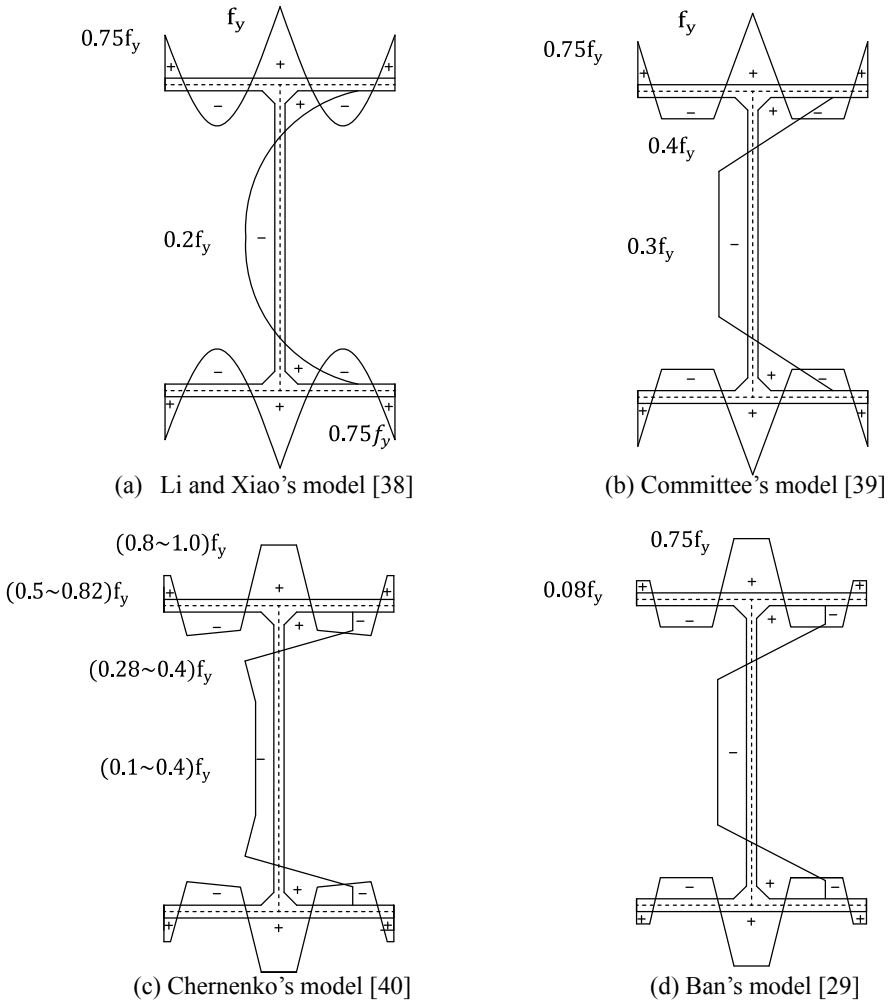

Figure 11. Existing models of residual stress for welded H-sections

7. RESIDUAL STRESS DISTRIBUTION MODEL

Residual stress distribution models are essential for the analysis and design of steel structural members. Figure 11 shows several existing models for welded H-sections. Chinese standard for steel structures [17] adopts Li and Xiao's model [38] and the model recommended by the code committee [39] for welded H-sections, which were mainly based on experiment tests on normal steel sections, regardless of steel grades and dimensions. Chernenko and Kennedy [40] proposed a residual stress distribution model after summarising available experimental data. Another model by Ban et al. [29] was based on the experimental tests on welded 460 MPa steel H-sections. In the model, tensile stresses were constant and compressive stresses were defined as a function of the plate thickness and width-to-thickness ratio.

In accordance with experimental results of welded Q345GJ steel H-sections, a residual stress model is proposed. Figures 12(a) and (b) show the data of residual stresses in the web and flanges. It is observed that the magnitude of residual stresses at the tip of flame-cut flanges is quite limited, ranging from $-0.18f_y$ to $0.18f_y$, much smaller than that suggested other models. Thus, a tensile stress value of $0.03f_y$ at the flange tip is suggested in the proposed model. In the flange, the mean value of peak tensile residual stresses is equal to $0.67f_y$, and the compressive residual stress is determined as $-0.22f_y$. In the web, the maximum tensile and compressive residual stresses are $0.96f_y$ and $-0.22f_y$, respectively.

The proposed model is significantly different from existing models in terms of the maximum tensile and compressive residual stresses in the flange, as shown in Figure 13. For instance, the peak tensile residual stress at the flange tip is only $0.03f_y$, much smaller than the values recommended by the Chinese code [17] ($0.75f_y$) and Chernenko and Kennedy [40] ($(0.5\sim0.82)f_y$) for normal steel. In the middle of the flange, the maximum tensile stress is $0.67f_y$, only 67% of the suggested value f_y. Similar results can also be obtained when comparisons are made among the compressive residual stresses in the flange. Nevertheless, limited differences exist between the residual stresses in the web calculated from the proposed and available models. It should be mentioned that the suggested residual stress distribution model is derived for welded Q345GJ H-sections with height-to-width ratios greater than 1.5 and plate thickness of about 10 mm. More experimental tests are needed for other welded H-sections.

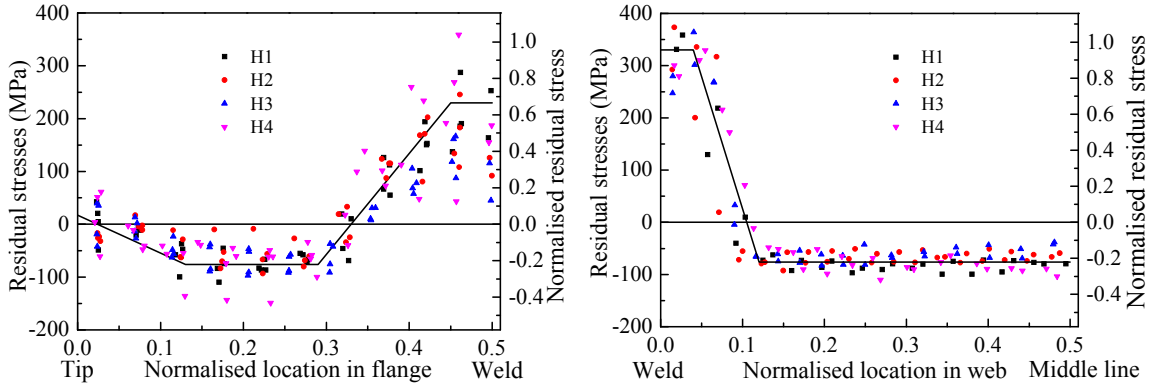

Figure 12. Residual stress distribution in the flange and web

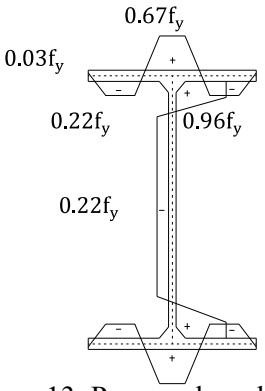

Figure 13. Proposed models of residual stress for welded H-sections

8. CONCLUSIONS

In this paper, the residual stress of four welded H-sections fabricated with flame-cut Q345GJ steel plates was investigated by using the sectioning method. For curved strips after sectioning, different curve correction methods were adopted. In addition to the circular correction method, straightening method was proposed to measure the total length of the middle-thickness layer. By using the methods, residual stresses in the web and flanges were calculated and a residual stress distribution model was developed for welded H-sections. The following conclusions were drawn from the study.

(1) Considerable differences exist between different curve correction methods, especially for curved strips after sectioning. Comparisons of the correction methods show that the parabolic and circular assumptions provide nearly the same results. However, the values are much larger than that calculated from the method by Tebedge and Tall [20].

(2) In the circular curve correction method, the residual stress at the middle-thickness layer of a strip can be determined from the measurements on one surface. However, it is highly sensitive to the strip thickness and strip offset value. Therefore, two surface measurements are still suggested to ensure the accuracy.

(3) Straightening method was proposed to measure the residual stresses in curved strips and the results were in good agreement with that obtained from the circular correction method. The closing error of residual stresses on each section was limited, indicating the accuracy of the proposed method for residual stress calculations. However, by using the straightening method, the number of measurements can be reduced by half. Besides, this method is particularly suitable for strips with large deformations.

(4) The residual stress profile in H-sections welded by Q345GJ steel plates with flame-cut edges was similar to that in welded normal steel H-sections. However, the peak tensile and compressive residual stresses in the flange were much lower than that given by existing models. Moreover, the tensile residual stresses close to welds were irrespective of sectional dimensions, while the compressive residual stresses were directly related to sectional dimensions.
Due to the differences in residual stresses in the flange, welded Q345GJ steel beams is expected to exhibit different behaviour from normal steel sections under vertical loads. Thus, further experimental tests are needed to evaluate the stability resistance of welded Q345GJ steel H-sections.

ACKNOWLEDGEMENTS

The authors gratefully acknowledge the financial supports provided by the National Natural Science Foundation of China (No. 51078368 and No. 50808185) and the Fundamental Research Funds for the Central Universities (No. CDJZR12200007).

REFERENCES

[1] Pocock, G., "High Strength Steel Use in Australia, Japan and the US", Structural Engineer, 2006, Vol. 84, No. 21, pp. 27-31.
[2] European Committee for Standardization, Eurocode 3: Design of steel structures: Part 1-12: Additional Rules for the Extension of EN 1993 up to Steel Grades S700, EN 1993-1-12, 2007.
[3] American Institute of Steel Construction, Specification for Structural Steel Buildings, ANSI/AISC 360-10, Chicago, Illinois, 2010.
[4] Standard Australia, Steel Structures, AS4100-1998, 1998.
[5] Graville, B.A., "Cold Cracking in Welds in HSLA Steels", International Conference on Welding of HSLA (Microalloyed) Structural Steels, American Society for Metals, 1976.
[6] Japanese Standards Association, Rolled Steel for Building Structure, JISG 3136, Tokyo, 2012.
[7] American Society for Testing and Materials, Standard Specification for Structural Steel Shapes, A922/A922M, West Conshohocken, PA, 2011.
[8] Bjorhovde, R., "Development and Use of High Performance Steel", Journal of Constructional Steel Research, 2004, Vol. 60, No. 3, pp. 393-400.
[9] Shi, Y.J., "Development and Application of High Strength and High Performance Steel in Buildings", The 3rd International Forum on Advances in Structural Engineering, Beijing, 2009.
[10] Stanardization Administration of China, Steel Plates for Building Structure, GB/T 19879-2005, Beijing, Standards Press of China, 2005 (in Chinese).
[11] Stanardization Administration of China, Carbon structural steels, GB/T 700-2006, Beijing, Standards Press of China, 2006 (in Chinese).
[12] Stanardization Administration of China, High strength low alloy structural steels, GB/T 1591-2008, Beijing, Standards Press of China, 2008 (in Chinese).
[13] Nie, S.D., Dai, G.X. and Yang, B., "Development and Application of High-performance GJ Steel in Construction Practices", The 9th National Modern Structure Conference, Jinan, 2009 (in Chinese).
[14] Fan, Z., Wu, X.M. and Yu, Y.Q., "Revised Preliminary Design of Steel Structure of National Stadium Beijing", Spatial Structures, 2005, Vol. 11, No. 3, pp. 3-13 (in Chinese).
[15] Chen, L.R., "The characteristics of structural steel for the main building in new location of China Central Television Station", Steel Structures, 2007, Vol. 22, No. 91, pp. 1-4 (in Chinese).
[16] Chen, L.R. and Chai, C., "Overview of Steel Consumption of Major Building Steel Structure Engineering", The 4th Symposium of China Steel Construction Association & National Steel Structural Congress 2006, Beijing, 2006 (in Chinese).
[17] Ministry of Construction, Code for design of steel structures, GB 50017-2003, Beijing, China Archetecture & Building Press, 2003 (in Chinese).
[18] Wei, M.Z., "Steel Structures", Wuhan University of Technology Press, 2000 (in Chinese).

[19] Ziemian, R.D., "Guide to Stability Design Criteria for Metal Structures", John Wiley & Sons, Inc, 2010.
[20] Tebedge, N., Alpsten, G. and Tall, L., "Residual-stress Measurement by the Sectioning Method", Experimental Mechanics, 1973, Vol. 13, No. 2, pp. 88-96.
[21] Wang, G.Z. and Zhao, W.W., "Residual Stress Measurement in Welded and Hot-rolled I section Steels", Industrial Construction, 1986, Vol. 16, No. 7, pp. 32-37 (in Chinese).
[22] Alpsten, G.A. and Tall, L., "Residual Stresses in Heavy Welded Shapes", Welding Research Supplement, 1970, Vol. 49, pp. 93-105.
[23] Rasmussen, K.J.R. and Hancock, G.J., "Tests of High Strength Steel Columns", Journal of Constructional Steel Research, 1995, Vol. 34, No. 1, pp. 27-52.
[24] Rasmussen, K.J.R. and Hancock, G.J., "Plate Slenderness Limits for High Strength Steel Sections", Journal of Constructional Steel Research, 1992, Vol. 23, No. 1, pp. 73-96.
[25] Wang, Y.B., Li, G.Q. and Chen, S.W., "The Assessment of Residual Stresses in Welded High Strength Steel Box Sections", Journal of Constructional Steel Research, 2012, Vol. 76, pp. 93-99.
[26] Wang, Y.B., Li, G.Q. and Chen, S.W., "Residual Stresses in Welded Flame-cut High Strength Steel H-sections", Journal of Constructional Steel Research, 2012, Vol. 79, pp. 159-165.
[27] Ban, H.Y., Shi, G. and Shi, Y.J., "Residual Stress Tests of High-strength Steel Equal Angles", Journal of Structural Engineering, 2012, Vol. 138, No. 12, pp. 1446-1454.
[28] Ban, H.Y., Shi, G., Shi, Y.J. and Wang, Y.Q., "Residual Stress of 460 MPa High Strength Steel Welded Box Section: Experimental Investigation and Modeling", Thin-Walled Structures, 2013, Vol. 64, pp. 73-82.
[29] Ban, H.Y., Shi, G., Bai, Y., Shi, Y.J. and Wang, Y.Q., "Residual Stress of 460 MPa High Strength Steel Welded I Section: Experimental Investigation and Modeling", International Journal of Steel Structures, 2013, Vol. 13, No. 4, pp. 691-705.
[30] Spoorenberg, R.C, Snijder, H.H., Cajot, L.G. and May, M.S., "Experimental Investigation on Residual Stresses in Heavy Wide Flange QST Steel Sections", Journal of Constructional Steel Research, 2013, Vol. 89, pp. 63-74.
[31] General Administration of Quality Supervision Inspection and Quarantine, Steel and steel products-Location and preparation of test pieces for mechanical testing, GB/T 2975-1998, Beijing, Standards Press of China, 1998 (in Chinese).
[32] Stanardization Administration of China, Metallic materials-Tensile testing-Part 1: Method of Test at Room Temperature, GB/T 228.1-2010, Beijing, Standards Press of China, 2010 (in Chinese).
[33] Ban, H.Y., Shi, G. and Xing, H.J., "Stability of Q420 High Strength Steel Equal-leg Angle Members under Axial Compression (I): Experimental Study on the Residual Stress", China Civil Engineering Journal, 2010, Vol. 43, No. 7, pp. 14-21 (in Chinese).
[34] Wang, Y.Q., Guan J., Zhang, Y., Shi, Y.J. and Yang, L., "Experimental Study on Residual Stress of Austenitic Stainless Steel 316 in Fabricated I-sections", Industrial Construction, 2012, Vol. 42, No. 5, pp. 44-50 (in Chinese).
[35] Cui, J., "Influence of Residual Stress on the Resistance of Welded I Sections Fabricated with Flame-cut Plates", Chongqing Institute of Archetecture and Engineering, Chongqing, 1983 (in Chinese).
[36] Sherman, D.R., "Residual Stress Measurement in Tubular Members", Journal of the Structural Division, 1969, Vol. 95, No. 4, pp. 635-647.
[37] Structural Stability Research Council, "Determination of Residual Stresses in Structural Shapes", Experimental Techniques, 1981, Vol. 5, No. 3, pp. 4-7.

[38] Li, K.X. and Xiao, Y.H., "Column Curves for Steel Compression Members", Journal of Chongqing Institute of Archetecture and Engineering, 1985, Vol. 1, pp. 24-33 (in Chinese).
[39] Committee for Code for Design of Steel Structures, Application of Code for Design of Steel Structures in China, Beijing, China Planning Press, 2003 (in Chinese).
[40] Chernenko, D.E. and Kennedy, D.J.L., "An Analysis of the Performance of Welded Wide Flange columns", Canadian Journal of Civil Engineering, 1991, Vol. 18, No. 4, pp. 537-555.